Combined 3-dimensional and mirror-image analysis for the diagnosis of asymmetry

Janalt Damstra,[a] Barbara Constance Maria Oosterkamp,[b] Johan Jansma,[c] and Yijin Ren[d]
Groningen, The Netherlands

Three-dimensional imaging techniques have greatly improved our ability to assess asymmetry by means of linear and angular measurements. However, visualizing deformities enables a unique appreciation of the underlying deformity, which might not be possible by looking at quantitative numbers alone. This article describes the method of a mirror-image analysis technique to visualize the asymmetry to assist in diagnosis and treatment planning. Other advantages of a mirror-image analysis, in addition to the quantitative analysis, are also discussed. (Am J Orthod Dentofacial Orthop 2011;140:886-94)

The development of computerized tomography (CT) has greatly reduced errors of frontal cephalometry and improved our ability to diagnose asymmetry and other craniofacial deformities.[1,2] Cone-beam CT (CBCT) was developed for 3-dimensional (3D) imaging of the maxillofacial area and has become popular in dentistry, orthodontics, and maxillofacial surgery.[3] The advantages of CBCT include less radiation exposure (than conventional CT), less artefact formation, and submillimeter spatial resolution.[3] CBCT has been shown to produce accurate 3D images of the craniofacial region and a 1-to-1 image-to-reality ratio, which is necessary for accurate detection of the underlying deformities and asymmetries.[4-8]

Recent literature has described new quantitative analyses to diagnose asymmetries on 3D CT or CBCT images.[1-3,9-14] Because quantitative measurement is a key element in diagnosis of asymmetry, 3D images are best suited for accurate diagnosis. Quantitative measurement provides important information for treatment planning; eg, it determines the target area for operation and the surgical method to be followed. However, by looking at quantitative numbers alone, it might not be possible to appreciate the extent of the underlying deformity. To overcome this limitation, Terajima et al[14] described a visual 3D method for analyzing the morphology of patients with maxillofacial deformities. They superimposed a standard 3D Japanese skeletal model on the patient's 3D CT images to show the underlying deformities. However, these 3D templates only satisfy the Japanese norms; this limits their clinical applications. We use a mirror image for visual analysis of the asymmetry. The mirror-image analysis does not rely on population norms and can therefore be used for the detection of asymmetries in all populations. A mirror image is a reflected duplication that appears identical but in reverse. By superimposition of the mirror image of the anatomically correct part of the anatomy over the deformity, the differences become visual and can also be quantified. The use of mirror images is not new in craniofacial imaging techniques. In maxillofacial surgery, the reverse models of 3D mirror-image templates have been described to correct and reconstruct various craniofacial abnormalities.[15,16]

The aims of this study were to illustrate and discuss the method of mirror-image analysis in addition to the quantitative 3D analysis of asymmetry with a case report. The advantages of the mirror-image analysis will also be discussed.

MATERIAL AND METHODS

A boy, aged 14 years, was referred to the Department of Orthodontics at the University of Groningen, Groningen, The Netherlands, as part of the multidisciplinary approach for treatment of Parry-Romberg syndrome. His medical history showed that noticeable asymmetry began at the age of 6 years, indicating early onset of

From University Medical Center Groningen, University of Groningen, Groningen, The Netherlands.
[a]Postgraduate student, Department of Orthodontics.
[b]Lecturer and staff orthodontist, Department of Orthodontics.
[c]Lecturer and staff maxillofacial surgeon, Department of Oral and Maxillofacial Surgery.
[d]Professor and chair, Department of Orthodontics.
The authors report no commercial, proprietary, or financial interest in the products or companies described in this article.
Reprint requests to: Janalt Damstra, Department of Orthodontics, University Medical Center Groningen, PO Box 30.001, Groningen, 9700 RB, The Netherlands; e-mail, j.damstra@dmo.umcg.nl.
Submitted, January 2010; revised and accepted, March 2010.
0889-5406/$36.00

doi:10.1016/j.ajodo.2010.03.032

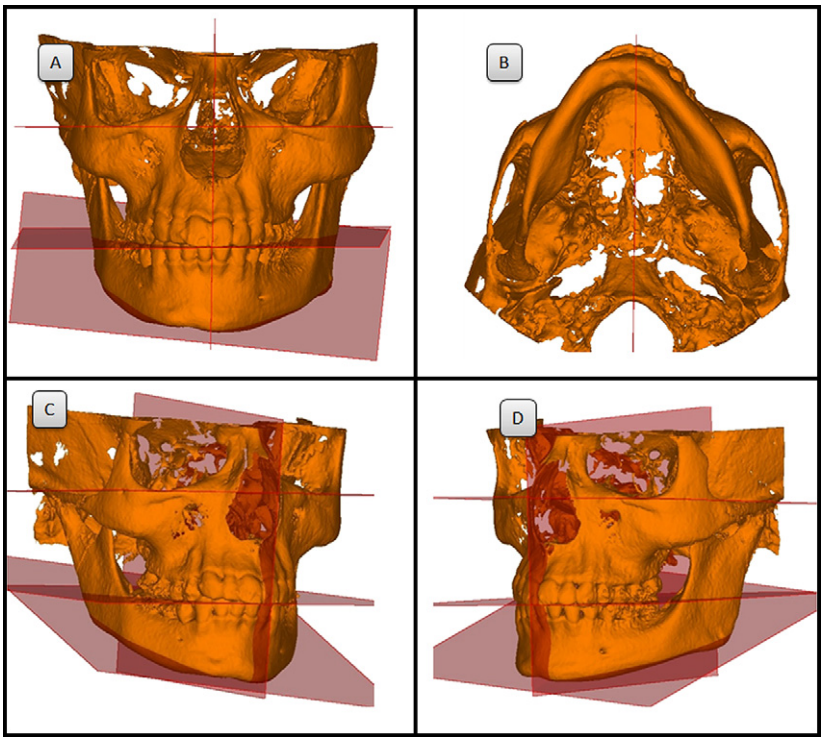

Fig 1. Three-dimensional surface model of the patient with early-onset Parry-Romberg syndrome: **A,** frontal view; **B,** inferior view; **C,** right lateral view; **D,** left lateral view.

the disease. The diagnosis of Parry-Romberg disease was made at the age of 7 years. The extraoral examination showed a marked asymmetry from atrophy of the right side of the face. The chin was deviated to the right, and deviation of the nose to the affected side was noticeable. The intraoral examination showed that the mandibular dental midline was rotated to the right. Delayed eruption of the mandibular premolars and molars was noted on the right side.

A CBCT image of the patient was acquired by using a KaVo 3D eXam scanner (KaVo Dental, Bismarckring, Germany). The image was made with a 17-cm field of view at a voxel resolution of 0.4 mm. The CBCT data set was exported in DICOM file format and imported into SimPlant Ortho Pro software (version 2.00; Materialise Dental, Leuven, Belgium). The 3D image was rendered, and surface models of the hard tissues were created with the software (Fig 1). To quantify the osseous changes, a 3D analysis was developed combining linear and angular measurements previously described.[1-3] The measurements used for the quantitative 3D analysis are illustrated in Figure 2 and described in Table I. Asymmetry was described by the right-side measurement subtracted from the left-side measurement.[1,2]

In addition to the quantitative 3D analysis, a mirror-image analysis was performed to visually analyze the extent of the atrophy and confirm the diagnosis. The method for the mirror image of the maxilla was as follows: the left unaffected side was mirrored along the midsagittal plane. The mirror image was then superimposed over the right affected side (Fig 3, *A-C*). The software allows for the surface models to become semitransparent and allows for movement of the models in all 3 planes of space. Visual inspection of the anterior and posterior cranial base confirmed the superimposition (Fig 3, *D*). For the mandible, a vertical plane through the spina mentalis, parallel to the midsagittal plane, was used because of the chin deviation (Fig 4, *A*). The left side was mirrored and superimposed over the right side (Fig 4, *A-C*). Visual inspection of the inner contour of the cortical plates of the inferior border of the symphysis confirmed the superimposition (Fig 4, *D*). For both the maxilla and mandible, the difference in volume was visualized with the software by means of a customized color scale (Figs 3, *F*, and 4, *F*). The measurement differences were used as a guide to determine the parameters of the color scales.

RESULTS

The quantitative results of the 3D cephalometric analysis are described in Table II. The smaller measurements indicate that the mandible and the maxilla were

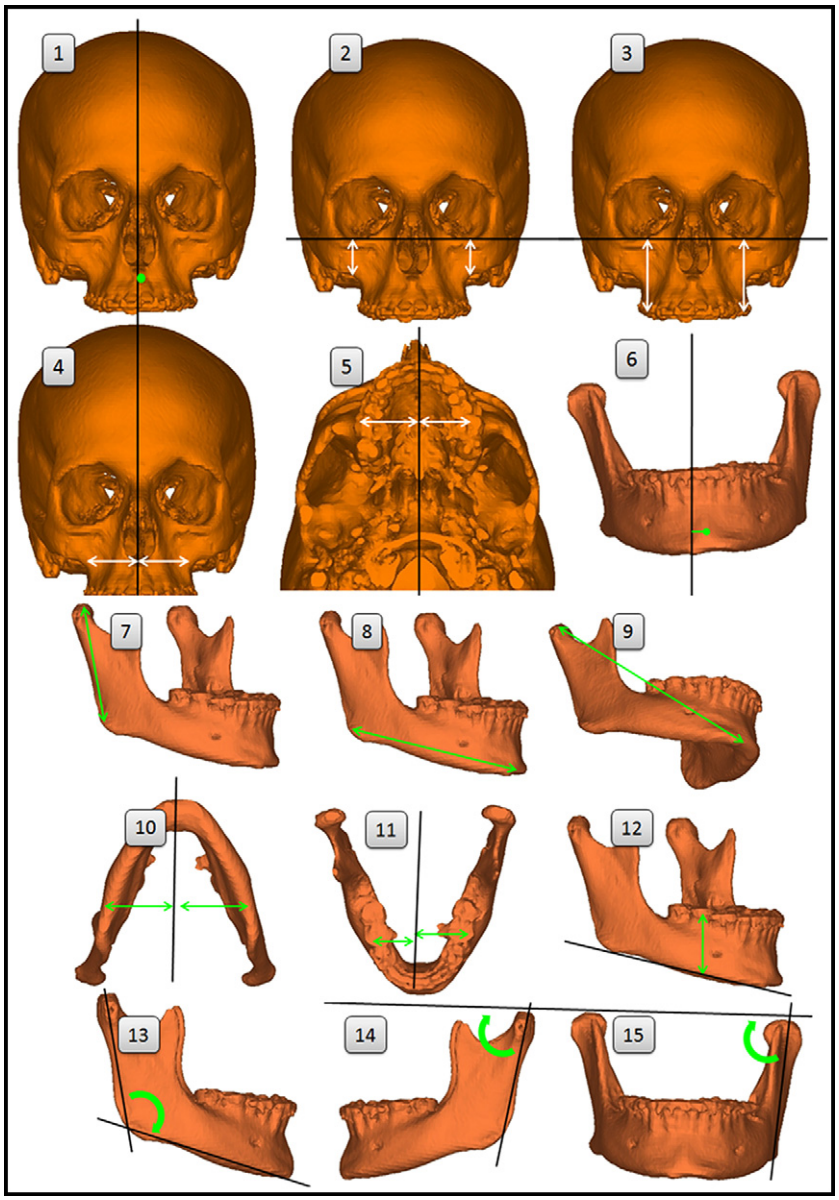

Fig 2. Measurements used for the quantitative analysis of asymmetry: *1*, Maxillary rotation; *2*, maxillary height; *3*, maxillary dental height; *4*, maxillary width; *5*, maxillary dental width; *6*, mandibular rotation; *7*, ramus length; *8*, mandibular body length; *9*, total mandibular length; *10*, mandibular width; *11*, mandibular dental width; *12*, mandibular dental height; *13*, gonial angle; *14*, lateral ramus inclination; *15*, frontal ramus inclination; *16*, facial width; 1*7*, occlusal cant; *18*, mandibular cant; *19*, total maxillary width and total mandibular width; *20*, condylar width.

affected on the right side. The facial width was 5 mm less on the right side compared with the left side. This indicates restricted growth of the zygomatic arch because of soft-tissue atrophy. The maxilla height was decreased on the right side (1.7 mm). However, there was no difference between the maxillary dental heights of the left and right sides, possibly because of the overeruption of the maxillary dentition from the delayed eruption of the posterior mandibular dentition.

The mandible was rotated 4.88 mm to the right. On the affected side, the mandibular body length was 10.3 mm shorter compared with the left side. The ramus was also 4.2 mm shorter on the affected side. The difference in the ramus length explains the significant cant of

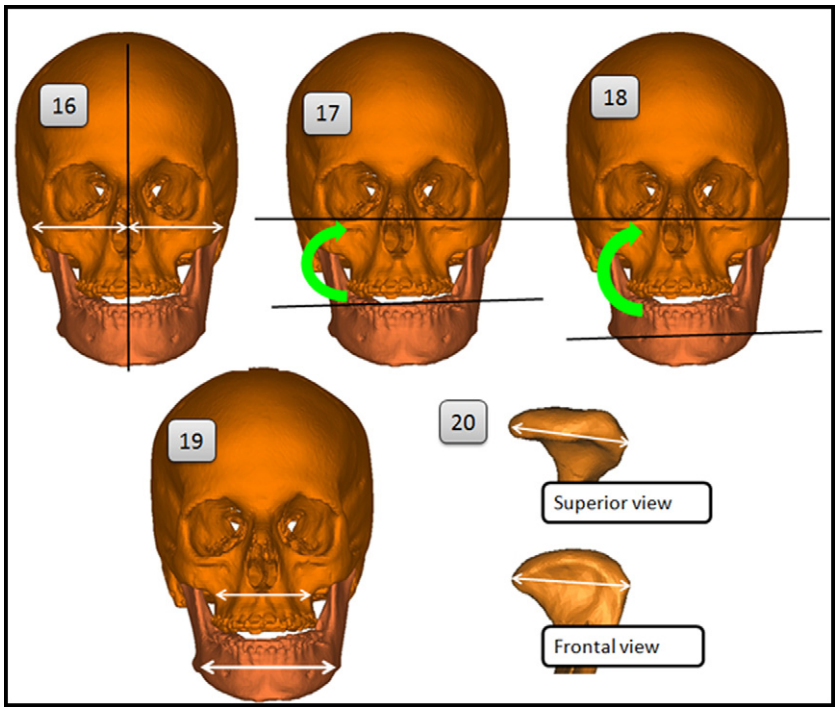

Fig 2. (continued).

the mandible (13.0°). The restrictive nature of the disease manifested not only as restriction of the lengths but also the angular development of the mandible. Most noticeable was the underdevelopment of the gonial angle on the right side; it was 113.0° on the left side compared with 125.9° on the right side. The lateral and frontal ramus inclinations were smaller on the right side (6.2° and 3.0°). Delayed eruption caused the underdevelopment of the alveolar process of the mandible (5.3 mm) and resulted in an occlusal cant. Interestingly, although the lower face of the affected side showed significant osseous changes, the condylar width dimensions were not different from the unaffected side.

The mirror-image technique visualized the findings of the quantitative 3D analysis regarding the hypoplasia of the zygomatic region and the mandible. The differences between the mirror image and the affected side were calculated and illustrated with color scales in Figures 3, *F*, and 4, *F*.

DISCUSSION

Parry-Romberg syndrome (or progressive hemifacial atrophy) is an uncommon degenerative condition characterized by a slow and progressive atrophy of facial tissues, muscles, bones, and skin.[17-26] The progressive atrophy of the facial tissues is often in stark contrast to the apparently normal contralateral side. The extent of the atrophy is usually limited to 1 side of the face. The osseous lesions described in Parry-Romberg syndrome appear to be related to the age at which the condition appears. With late onset of the condition after the age of 15 years, the lesions appear exclusively in the soft tissues.[24] Restriction of skeletal growth from the soft-tissue atrophy of early-onset Parry-Romberg syndrome has been previously reported. However, Duymaz et al[26] reported no osseous changes of the craniofacial region after 3D CT examination of a patient with early-onset Parry-Romberg syndrome. In our patient, early onset of the atrophy resulted in hypoplasia of the fronto-orbitozygomatic region, mandibular rotation, and underdevelopment of the mandible in all dimensions of space. This is in contrast to the findings of Duymaz et al. It would, however, be incorrect to draw conclusions from 1 case report because the osseous changes might be different from person to person. This is because involvement can stabilize at any stage of growth and development, and patients who manifest atrophy earlier have greater repercussions.[24] Future studies will investigate a larger group of patients with early-onset Parry-Romberg syndrome by means of 3D analysis to fully determine the characteristics of early-onset soft-tissue atrophy on the middle and lower face.

The mirror-image analysis performed in addition to the quantitative 3D analysis proved to be valuable. Not

Table I. Reference planes and measurements used for this analysis

Reference planes	*Description*
1. Midsagittal	Plane that passes through nasion and the constructed midpoint between the lateral points of the foramen magnum and the constructed midpoint between the left and right clinoid processes
2. Frankfort horizontal	Plane that passes through both orbitale landmarks and through the mean of the 2 porion landmarks
3. Occlusal	Plane that passes through the midpoint of the maxillary incisor tip and mandibular incisor tip landmarks, the midpoint of the maxillary right first molar mesial cusp and the mandibular right first molar mesial cusp and the mean of the maxillary left first molar mesial cusp and the mandibular left first molar mesial cusp
4. Mandibular	Plane that passes through both gonion landmarks and menton
Measurements	*Description (distance or angle)*
1. Maxillary rotation	Point A to the midsagittal plane
2. Maxillary height	Jugulare to the Frankfort horizontal plane
3. Maxillary dental height	Mesial cusp tip of the maxillary first molar to the Frankfort horizontal plane
4. Maxillary width	Jugulare to the midsagittal plane
5. Maxillary dental width	Mesial cusp tip of the maxillary first molar to the midsagittal plane
6. Mandibular rotation	Pogonion to the midsagittal plane
7. Ramus length	Condylion to gonion
8. Body length	Gonion to menton
9. Total mandibular length	Condylion to menton
10. Mandibular width difference	Antegonion to the midsagittal plane
11. Mandibular dental width difference	Mesial cusp tip of the mandibular first molar to the midsagittal plane
12. Mandibular dental height difference	Mesial cusp tip of the mandibular first molar to the mandibular plane
13. Gonial angle	Angle between a line that connects the landmarks of gonion and condylion and a line that connects gonion and menton
14. Lateral ramus inclination	Angle between the Frankfort horizontal plane and a line formed by connecting the landmarks of gonion and condylion from the lateral view
15. Frontal ramus inclination	Angle between the Frankfort horizontal plane and a line formed by connecting the landmarks of gonion and condylion from the frontal view
16. Facial width	Zygion to the midsagittal plane
17. Occlusal cant	Angle between the Frankfort horizontal plane and a line connecting the maxillary left and right first molar cusps
18. Mandibular cant	Angle between the Frankfort horizontal plane and a line connecting the left and right antegonion landmarks
19. Maxillary total width	Jugulare left to jugulare right
Mandibular total width	Antegonion left to antegonion right
20. Condylar width	Most lateral point of the condylar head to the most medial point of the condylar head

only did it confirm the diagnosis derived from quantitative measurements, but it also helped to reduce diagnostic errors when relying on numbers alone. It does not rely on normative values, it creates new appreciation of osseous changes because the differences can be depicted as volumes rather than numbers, it helps in development of treatment strategies, and it improves communications between orthodontists and maxillofacial surgeons. Perhaps the most valuable contribution of the visual analysis is that it has been an excellent tool to explain the extent of the osseous changes to patients to further their understanding of the disease and the possibilities and limitations of the treatment. It is therefore recommended to perform a mirror-image analysis in addition to quantitative analyses in patients with asymmetries to enable a unique appreciation of the underlying deformity that might not be possible by studying quantitative numbers alone.

Importantly, where there is unilateral growth of the mandible, it will have a tendency to rotate toward the area of less growth and cause chin deviation. Therefore, it is debatable whether the mandible can be divided into affected and unaffected sides because the unaffected side is always indirectly affected. As a result of rotation, the ramus inclinations on both sides might be affected. The chin deviation also excludes the use of the midsagittal plane, and the mandible should be divided and mirrored with a vertical plane through the spina mentalis.

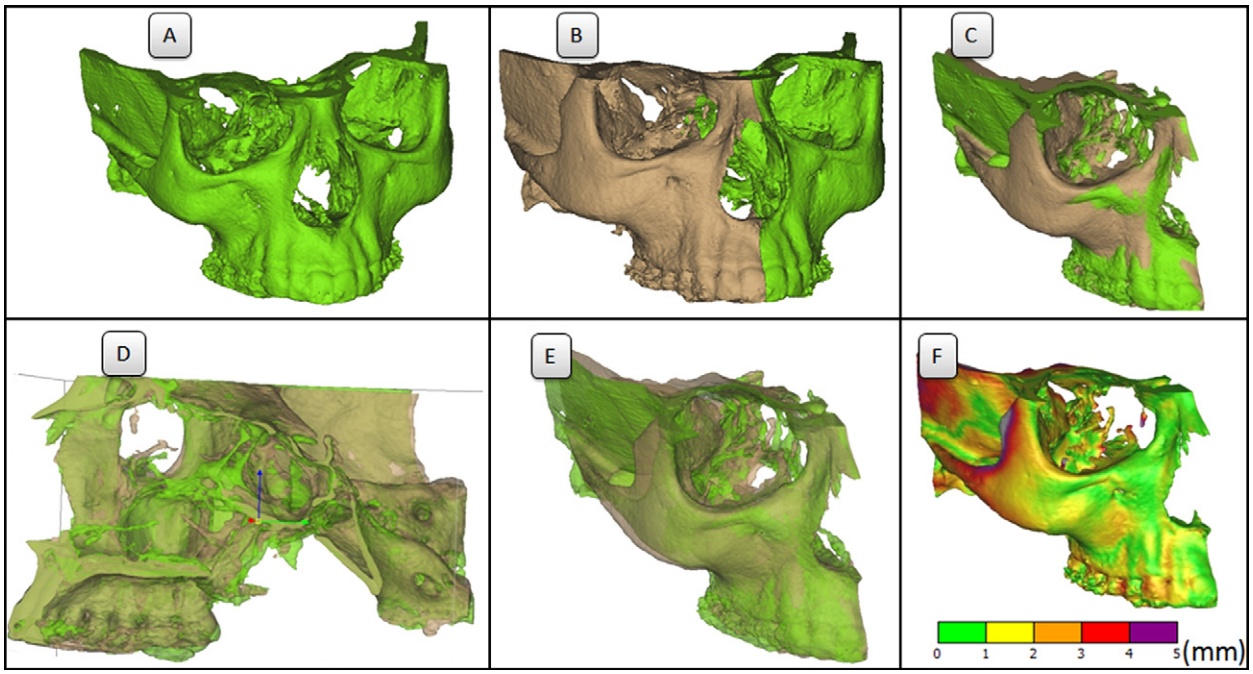

Fig 3. Mirror-image analysis of the maxilla: **A-C,** the left side of the maxilla is mirrored (*brown*) over the original right surface model (*green*) along the midsagittal plane; **D,** the superimposition is adjusted to best fit along the cranial base if necessary; **E,** final superimposition with the surface models is semitransparent to visualize the differences; **F,** the differences of the mirror image and the original surface model are calculated and expressed with a customized color scale (in millimeters).

The effect of unilateral growth of the mandible is illustrated in Figure 5. Therefore, it is important to realize that mirror-image analysis is unlikely to give an accurate representation of the ramus inclinations when there is chin deviation. However, the differences in mandibular body length, ramus length, and gonial angle differences can be accurately determined with a mirror-image analysis (Fig 4, *E*).

In the literature, there seem to be great variations concerning the vertical axis or the midsagittal plane for analysis of asymmetry.[2,3,11,13,27] Jacobson[3] defined the midsagittal plane as a midline plane bisecting the head sagittally when viewing the patient from the front. He used nasion, the midpoint of the frontonasal suture, as the reference point. Grummons and Kappeyne van de Coppello[27] used a midsagittal line through crista galli and anterior nasal spine. Tuncer et al[13] used a plane through nasion, sella, and anterior nasal spine as the midsagittal plane for their 3D analysis. Harvold[28] reported that a line through nasion and anterior nasal spine represented the midsagittal line in more than 90% of patients. Baek et al[2] used the most superior edge of the crista galli and the midpoint between the anterior clinoid processes to construct a midsagittal plane perpendicular to the Frankfort horizontal plane. However, the anterior nasal spine and the Frankfort horizontal plane might not be accurate when there is asymmetry of the upper and midfacial regions.[14,29] In addition, we experienced variations in the midsagittal plane due to landmark identification differences of orbitale and porion when using the method of Baek et al.[2] The midpoint between the foramina spinosum (ELSA)[30] was considered the reference point, but we found that the foramina was not always clear on the CBCT images. To construct the midsagittal plane, we used nasion, the midpoint between the anterior clinoid processes, and the midpoint between the most lateral points on the foramen magnum (Fig 6). The advantages of this method are that the landmarks are easily identifiable on the CBCT images, and the accuracy of the midsagittal plane does not rely on the accuracy of other planes: eg, the Frankfort horizontal plane and the midsagittal plane are not influenced by upper and midfacial deformities. However, recently published literature suggests that a morphometrically determined midsagittal plane that eliminates the problems related to anatomical planes might therefore be more appropriate in describing the midsagittal plane of skeletal asymmetry.[31]

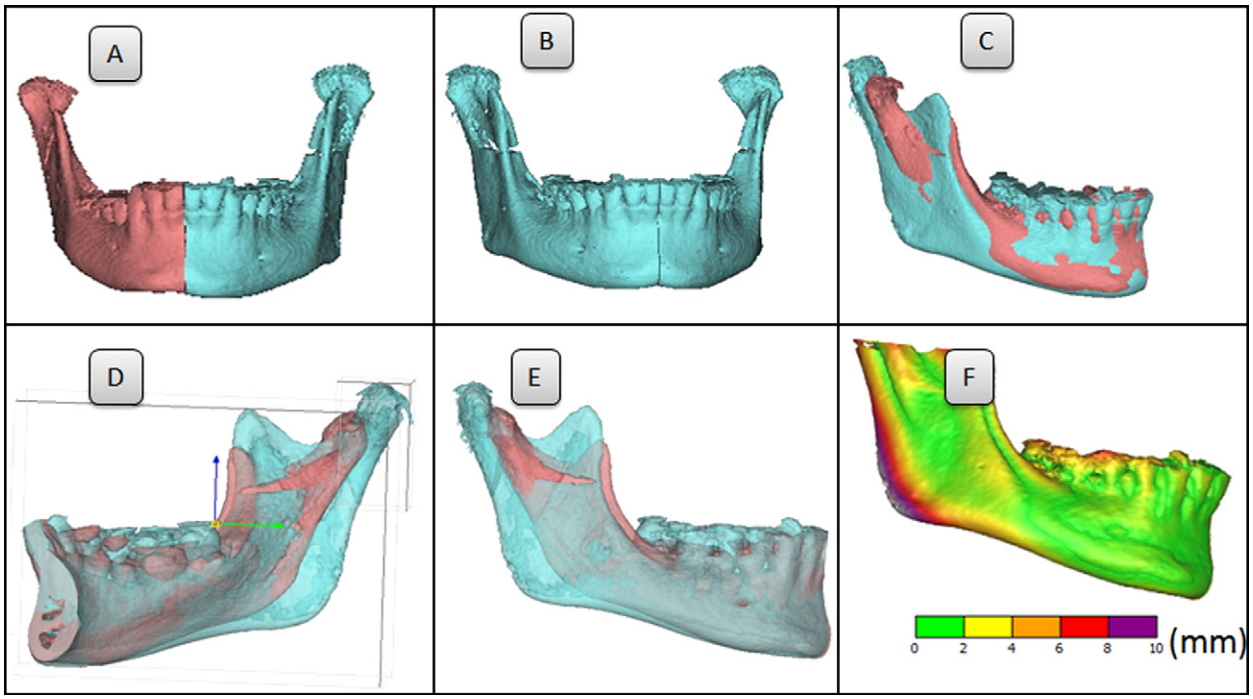

Fig 4. Mirror-image analysis of the mandible: **A-C,** the left side of the mandible is mirrored (*blue*) over the right original surface model (*pink*) along the vertical plane through menton; **D,** the superimposition is adjusted to best fit along the inner contour of the cortical plates of the inferior border of the symphysis if necessary; **E,** final superimposition with the surface models is semitransparent to visualize the differences; **F,** the differences of the mirror image and the original surface model are calculated and expressed with a customized color scale (in millimeters).

Table II. Results of the quantitive 3D analysis, with asymmetry defined as the right side subtracted from the left side

Maxilla	*Right*	*Left*	*Asymmetry*
1. Maxillary rotation (mm)	0.2		
2. Maxillary height difference (mm)	21.0	22.5	1.5
3. Maxillary dental height difference (mm)	42.4	41.9	−0.5
4. Maxillary width difference (mm)	34.1	33.1	−1.0
5. Maxillary dental width difference (mm)	27.1	26.1	−1
Mandible			
6. Mandibular rotation (mm)	4.88		
7. Ramus length difference (mm)	47.4	52.3	4.9
8. Body length difference (mm)	73.9	84.2	10.3
9. Total length difference (mm)	108.7	115.2	6.5
10. Mandibular width difference (mm)	42.6	43.7	1.1
11. Mandibular dental width difference (mm)	23.4	22.6	−0.8
12. Mandibular dental height difference (mm)	19.2	24.5	5.3
13. Gonion angle difference (°)	125.9	113.0	−12.9
14. Lateral ramus inclination difference (°)	78.0	82.2	6.2
15. Frontal ramus inclination difference (°)	85.0	88.0	−3.0
	Other		
16. Occlusal cant (°)	1.0		1.0
17. Mandibular cant (°)	13.0		13.0
18. Mandibular width-maxillary width (mm)	80.0	67.0	13.0
19. Facial width difference (mm)	54.4	59.4	5.0
20. Condyle width difference (mm)	18.27	18.07	−0.20

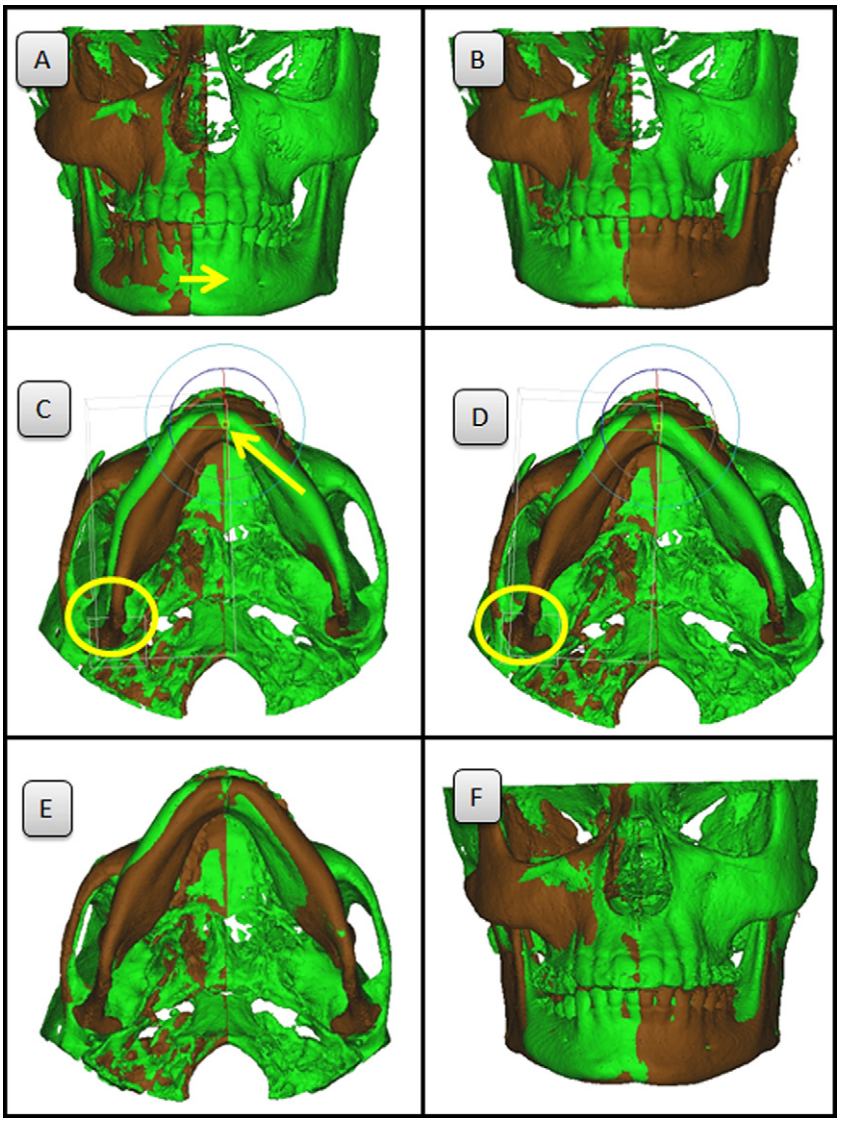

Fig 5. The effects of unilateral mandibular growth: **A,** the maxilla is mirrored along the midsagittal plane and the mandible through the spina mentalis; **B,** the plane through spina mentalis is aligned with the midsagittal plane to correct the chin deviation (*yellow arrow* indicates planned movement for alignment); **C,** with a rotation point on menton (*yellow arrow*); **D,** both mandibular halves (*brown*) are rotated to align the condylar heads in the fossa (*yellow circles*); **E,** inferior view, and **F,** frontal view illustrate the ideal positions of the mandible and maxilla (*brown*) compared with the original (*green*). Unilateral growth of the mandible affects the left and right sides when rotation occurs.

CONCLUSIONS

We introduced a new method for visualizing asymmetries. The combined 3D and mirror-image analysis was useful to visualize and better understand the osseous changes. The mirror-image analysis is useful to confirm the diagnosis derived from the quantitative results and assists in 3D treatment planning. The combined analysis showed that early-onset Parry-Romberg syndrome caused rotation of the mandible, hypoplasia of all dimensions of the mandible, and hypoplasia of the zygomatic region and the zygomatic arch.

REFERENCES

1. Hwang HS, Hwang CH, Lee KH, Kang BC. Maxillofacial 3-dimensional image analysis for the diagnosis of facial asymmetry. Am J Orthod Dentofacial Orthop 2006;130:779-85.

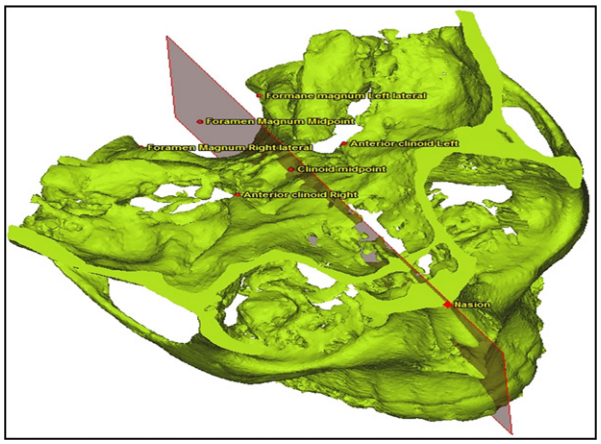

Fig 6. The landmarks and constructed midpoint landmarks used for the construction of the midsagittal plane.

2. Baek SK, Cho IS, Chang YI, Kim MJ. Skeletodental factors affecting chin point deviation in female patients with Class III malocclusion and facial asymmetry: a three dimensional analysis using computed tomography. Oral Surg Oral Med Oral Pathol Oral Radiol Endod 2007;104:628-39.
3. Jacobson RL. Three-dimensional cephalometry. In: Jacobson A, Jacobson RL, editors. Radiographic cephalometry: from basics to 3-D imaging. 2nd ed. Hanover Park, Ill: Quintessence; 2006. p. 233-47.
4. Damstra J, Fourie Z, Huddleston Slater JJR, Ren Y. Accuracy of linear measurements from cone-beam computed tomography-derived surface models of different voxel sizes. Am J Orthod Dentofacial Orthop 2010;137:16.e1-6.
5. Lagravère MO, Carey J, Toogood RW, Major PW. Three-dimensional accuracy of measurements made with software on cone-beam computed tomography images. Am J Orthod Dentofacial Orthop 2008;134:112-6.
6. Hassan B, van der Stelt P, Sanderink G. Accuracy of three-dimensional measurements obtained from cone beam computed tomography surface-rendered images for cephalometric analysis: influence of patient scanning position. Eur J Orthod 2008;31:129-34.
7. Brown AA, Scarfe WC, Scheetz JP, Silveira AM, Farman AG. Linear accuracy of cone beam CT 3D images. Angle Orthod 2009;79:150-7.
8. Mischkowski RA, Pulsfort R, Ritter L, Neugebauer J, Brochhagen HG, Keeve E, et al. Geometric accuracy of a newly developed cone-beam device for maxillofacial imaging. Oral Surg Oral Med Oral Pathol Oral Radiol Endod 2007;104:551-9.
9. Park SH, Yu HS, Kim KD, Lee KJ, Baik HS. A proposal for a new analysis of craniofacial morphology by 3-dimensional computed tomography. Am J Orthod Dentofacial Orthop 2006;129:600.e23-34.
10. Haraguchi S, Takada K, Yasuda Y. Facial asymmetry in patients with skeletal Class III deformity. Angle Orthod 2002;72:28-35.
11. Cho HJ. A three-dimensional cephalometric analysis. J Clin Orthod 2009;43:235-52.
12. Maeda M, Katsumata A, Ariji Y, Maramatsu A, Yoshida K, Goto S, et al. 3D-CT evaluation of facial asymmetry in patients with maxillofacial deformities. Oral Surg Oral Med Oral Pathol Oral Radiol Endod 2006;101:652-7.
13. Tuncer BB, Atac MS, Yuksel S. A case report comparing 3-D evaluation in the diagnosis and treatment planning of hemimandibular hyperplasia with conventional radiography. J Craniomaxillofac Surg 2009;37:312-9.
14. Terajima M, Nakasima A, Aoki Y, Goto TK, Tokumori K, Mori N, et al. A 3-dimensional method for analyzing the morphology of patients with maxillofacial deformities. Am J Orthod Dentofacial Orthop 2009;136:857-67.
15. Zhou L, He L, Shang H, Lui G, Zhoa J, Lui Y. Correction of hemifacial microsomia with the help of mirror imaging and rapid prototyping technique: a case report. Br J Oral Maxillofac Surg 2009;47:486-8.
16. Lee JW, Fang JJ, Chang LR, Yu CK. Mandibular defect reconstruction with the help of mirror imaging coupled with laser stereolithographic modeling technique. J Formos Med Assoc 2007;106:244-50.
17. Mazzeo N, Fisher JG, Mayer MH, Mathieu GP. Progressive hemifacial atrophy (Parry-Romberg syndrome). Case Report. Oral Surg Oral Med Oral Pathol Oral Radiol Endod 1995;79:30-5.
18. Lakhani PK, David TJ. Progressive hemifacial atrophy with scleroderma and ipsilateral limb wasting (Parry-Romberg syndrome). J R Soc Med 1984;77:138-9.
19. Gomez-Diez S, Lopez LG, Escobar ML, Gutierrez LJ, Oliva NP. Progressive facial hemiatrophy with associated osseous lesions. Med Oral Patol Oral Cir Bucal 2007;12:E602-4.
20. Miller MT, Sloane H, Goldberg MF, Grisolano J, Frenkel M, Mafee MF. Progressive hemifacial atrophy (Parry-Romberg disease). J Pediatr Ophthalamol Strabismus 1987;24:27-36.
21. Neville BW, Damm DD, Allen CN, Bouquot JE, editors. Patologica oral e maxilofacial. Rio de Janeiro, Brazil: Guanabara Koogan; 1998. p. 85.
22. Moore WH, Wong KS, Proudman TW, David DJ. Progressive hemifacial atrophy (Romberg's disease): skeletal involvement and treatment. Br J Plast Surg 1993;46:39-44.
23. Pinheiro TP, Silva CC, Silveira CS, Botelho PC, Pinheiro MG, Pinheiro JJ. Progressive hemifacial atrophy–case report. Med Oral Patol Oral Cir Bucal 2006;11:E112-4.
24. Zafarulla MY. Progressive hemifacial atrophy: a case report. Br J Ophthalmol 1985;69:669-76.
25. Asher S, Berg BO. Progressive hemifacial atrophy: report of three cases, including one observed over 43 years and computer tomographic findings. Arch Neurol 1982;39:44-6.
26. Duymaz A, Karabekmez FE, Keskin M, Tosun Z. Parry-Romberg syndrome: facial atrophy and its relationship with other regions of the body. Ann Plast Surg 2009;63:457-61.
27. Grummons DC, Kappeyne van de Coppello MA. A frontal asymmetry analysis. J Clin Orthod 1987;21:448-65.
28. Harvold E. Cleft lip and palate: morphological studies of the facial skeleton. Am J Orthod 1954;40:493-506.
29. Athanasios A, Van der Meij AJW. Posteroanterior (frontal) cephalometry. In: Athanasios A, editor. Orthodontic cephalometry. London, United Kingdom: Times Mirror International Publishers; 1995. p. 141-62.
30. Lagravère MO, Major PW. Proposed reference point for 3-dimensional cephalometric analysis with cone-beam computerized tomography. Am J Orthod Dentofacial Orthop 2005;128:657-60.
31. Damstra J, Fourie Z, De Wit MF, Ren Y. A three-dimensional comparison of a morphometric midsagittal plane to cephalometric midsagittal planes for craniofacial asymmetry. Clin Oral Investig 2011. doi:10.1007/s00784-011-0512-4.